İSTANBUL UNIVERSITY CERRAHPAŞA

ORIGINAL ARTICLE
Electrica 2021; 22(1): 101-108

Current Reconstruction for PMSM Drives Using a DC-Link Single Current Sensor

Mustafa Aktaş, Barış Çavuş

Department of Electrical-Electronics Engineering, Ondokuz Mayıs University, Faculty of Engineering, Samsun, Turkey

Cite this article as: M. Aktaş and B. Çavuş, "Current Reconstruction for PMSM Drives using a DC-link Single Current Sensor," *Electrica*, 22(1), 101-108, Jan. 2022.

ABSTRACT

This article presents field-oriented control of permanent magnet synchronous motor (PMSM) with single current sensor (DC-link). Field-oriented control requires current values flowing from three phases of the motor. These currents can be determined by current sensors to be connected to the phases as well as DC-link current sensor to be connected to supply side of invertor. Only one current value is determined by DC-link sensor. In this method, current reconstruction method is used to determine the current flowing from three phases. In this study, two different methods were compared. The mean value method and the least squares method were used to determine the current flowing through three phases using the current value measured from the DC-link current sensor. Performance evaluation of these two methods was made by comparing the integral squared error and total harmonic distortion values of the three phase currents obtained.
***Index Terms*—**Current reconstruction, DC-link sensor, field-oriented control, least squares method, permanent magnet synchronous motor (PMSM).

I. INTRODUCTION

Permanent magnet synchronous motor (PMSM) is widely used in industry as well as in applications such as automotive and robotics [1,2]. Small size, high speed response, low inertia, and no need for maintenance can be considered as the reasons for the widespread use of PMSM [3]. In addition, in recent years, price of materials in PMSM such as magnets has decreased [4]. Compared to other machines, advanced control strategies such as DTC can be easier to apply to PMSM [5].

PMSM must be driven with advanced control methods because this machine has undesirable effects. If PMSM is derived directly, as it starts to work, it draws high current from the source, has a low dynamic response, and has a large error in the steady-state operation. As a result, advanced control method such as field-oriented control (FOC) must be used to obtain efficiency and good dynamic performance [6,7]. Using FOC, the torque and flux vectors of PMSM can be controlled separately, as in the control of separated excited DC motor [8,9]. Blashke proposed FOC in 1971 [10]. In FOC, two phase variables (currents and fluxes) of PMSM are obtained from three phase variables, and this calculation is performed by using park transformation. Flux and torque control of PMSM are realized by using these two phases obtained as a result of park transformation. Therefore, mathematical model of three-phase PMSM can be written like a separated exited DC motor. Thus, control of torque and speed of PMSM can be realized easily [11,12]. FOC method has some advantages such as low ripple in flux and torque, low switching frequency, and high stable operation.

Three phase currents flowing through the stator phases are required for motor control. These three phase currents in stator windings are determined by the sensors. Currents in three-phase windings can be determined with the current sensors to be connected to two or three phases as well as a single sensor (DC-link) to be connected to the supply side of the inverter. With this technique, the number of current sensors can be reduced, so cost of the current sensor to be used is decreased [13,14]. In addition, measurement noise is reduced with this method [15]. With the DC-link current sensor, complexity of the system is reduced, and it enables protection of drive system against some faults [16]. Although just one current value is read with the DC-link current sensor, three phase current values are required for FOC. This problem is solved by current reconstruction methods.

Corresponding Author:
Bariş Çavuş

E-mail:
baris.cavus@omu.edu.tr

Received: February 12, 2021

Accepted: August 11, 2021

Available Online Date: September 27, 2021

DOI: 10.5152/electrica.2021.21015

One phase current is determined with DC-link current sensor and other two phase currents can be calculated by current reconstruction methods. Which phase current is read by DC-link sensor is determined by inverter topology and applied voltage vector. There are some studies in the literature that make vector control of PMSM using DC-link current sensor [17-24]. In Rieder et al. [17] and Piippo et al. [18], the operation of the speed sensorless PMSM with the DC-link current sensor is realized. In Yeom et al. [19], new mathematical method for current reconstruction is used. In Ahmed et al. [20], the maximum torque per ampere operation of PMSM is performed with DC-link current sensor. In Kraemer et al. [21], the operation of PMSM with DC-link current sensor is carried out with linear parameter varying. In Li et al. [22], fault detection and isolation study of PMSM is carried out with DC-link current sensor. In Lu et al. [23], the novel phase current reconstruction scheme without using null switching states is proposed. In Wang et al. [24], a new current regeneration method is proposed by moving the position of the single current sensor (SCS) from the DC bus to a current branch.

In this study, simulation of FOC of PMSM has been done in MATLAB M-file. Using PMSM and FOC's equations, PMSM's FOC control is modeled in MATLAB M-file environment. Three phase stator currents required for the FOC were obtained using the DC-link current sensor and curve-fitting algorithms. In this study, two simple and easy to apply current reconstruction methods are proposed. Two different curve-fitting methods, which are mean value method and least squares methods, have been developed. At the end of the study, the reconstructed current and real phase current graphs were obtained for the two curve-fitting methods. In order to make a good comparison of the two methods, harmonic analysis of motor currents was made. In addition, for both methods, the integral squared error (ISE) value was calculated using error between the reconstructed and measured currents.

II. FIELD-ORIENTED CONTROL OF PMSM

A. Mathematical Model of PMSM

PMSM comprises two parts (a rotor and three phase stator windings). Three phase voltage is applied to stator windings, and rotational magnetic field is generated by these windings. In addition, rotor has permanent magnets and these magnets produce rotor magnetic field. The rotor magnetic field follows rotating magnetic field generated by the stator windings and so PMSM runs [24]. Dynamic equations of PMSM can be written as below [25]:

$$\frac{di_d}{dt} = -\frac{R}{L_d} i_d + \frac{\omega_r L_q i_q}{L_d} + \frac{V_d}{L_d} \tag{1}$$

$$\frac{di_q}{dt} = -\frac{R}{L_q} i_q - \frac{\omega_r L_d i_d}{L_q} - \frac{\psi_m}{L_q} + \frac{V_q}{L_q} \tag{2}$$

$$\psi_d = L_d I_d + \psi_m \tag{3}$$

$$\psi_q = L_q I_q \tag{4}$$

$$T_e = \frac{3p}{2}\left(\psi_m I_q + \left(L_d - L_q\right) I_d I_q\right) \tag{5}$$

$$\frac{d\omega_r}{dt} = \frac{1}{J}\left(T_e - B\omega_r - T_L\right) \tag{6}$$

Equations (1)–(6) can be solved with numerical solution methods, and simulation of PMSM can be realized. In the equations given above, V_d and V_q are d and q components of stator voltage, I_d and I_q are d and q components of stator current, ψ_d and ψ_q are d and q components of stator flux, ψ_m is flux value of permanent magnet, T_e is induced torque, T_L is load torque, and ω_r is rotor speed. The parameters of the PMSM used in this study are given in Table I.

B. Field-Oriented Control

There are some advanced altertative current (AC) motor control strategies in application. One of the most successful methods in these strategies for the control of PMSM is the FOC. Fig. 1 shows the block diagram of classical FOC. As it can be seen in Fig. 1, torque reference is calculated using Proportional-Integral (PI) controller and the speed error, which is the difference between the reference speed and the actual motor speed. d component of the reference current can be calculated using reference flux and the torque. Additionally, transformation angle and q component of the reference current are calculated by using these two reference values. Three phase reference currents are calculated using Park transformation and d and q components of reference currents. Park transformation can be written as follows:

$$\begin{bmatrix} i_a \\ i_b \\ i_c \end{bmatrix} = \sqrt{\frac{2}{3}} \begin{bmatrix} \sqrt{\frac{1}{2}} & \cos(\theta) & -\sin(\theta) \\ \sqrt{\frac{1}{2}} & \cos\left(\theta - \frac{2\pi}{3}\right) & -\sin\left(\theta - \frac{2\pi}{3}\right) \\ \sqrt{\frac{1}{2}} & \cos\left(\theta + \frac{2\pi}{3}\right) & -\sin\left(\theta + \frac{2\pi}{3}\right) \end{bmatrix} \begin{bmatrix} i_0 \\ i_d \\ i_q \end{bmatrix} \tag{7}$$

The reference currents and actual motor currents flowing in stator windings are compared, and current error signals for each phase are obtained. Switching signals are obtained using the current error signal and hysteresis controller. Consequently, switching signals are applied to inverter, and PMSM runs in desired speed and torque [26].

TABLE I. PARAMETERS OF PERMANENT MAGNET SYNCHRONOUS MOTOR

Power	1.1 kW
Nominal torque	3 Nm
Nominal speed	3000 rpm
Pole number	8
Stator resistance	2.875 Ω
d axis inductance	8.5 mH
q axis inductance	8.5 mH
Magnet flux linkage	0.175 Wb
Inertia	0.0008 kgm^2

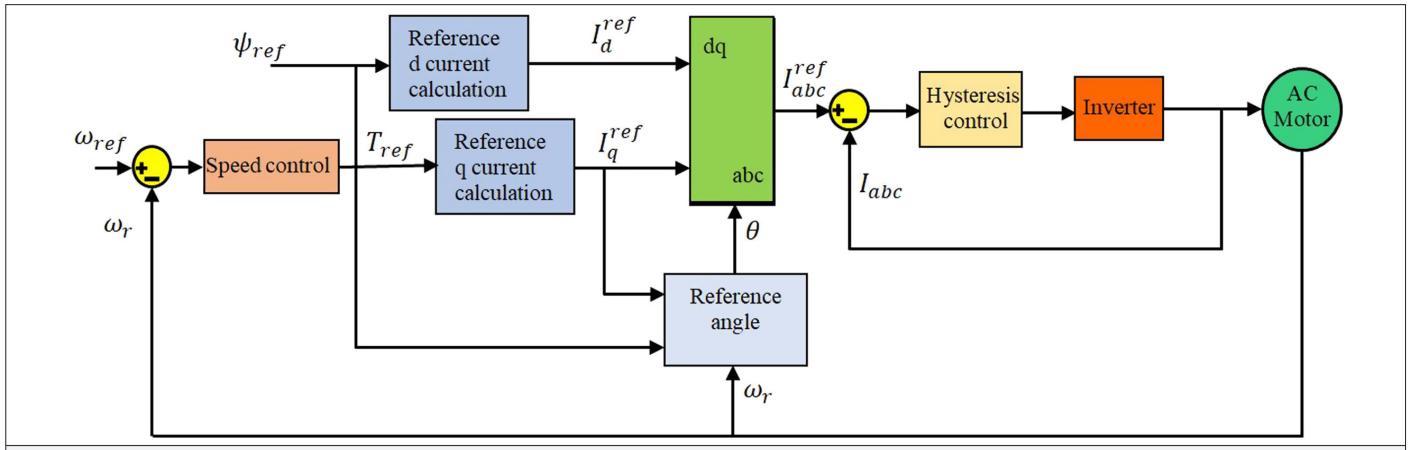

Fig. 1. FOC block diagram.

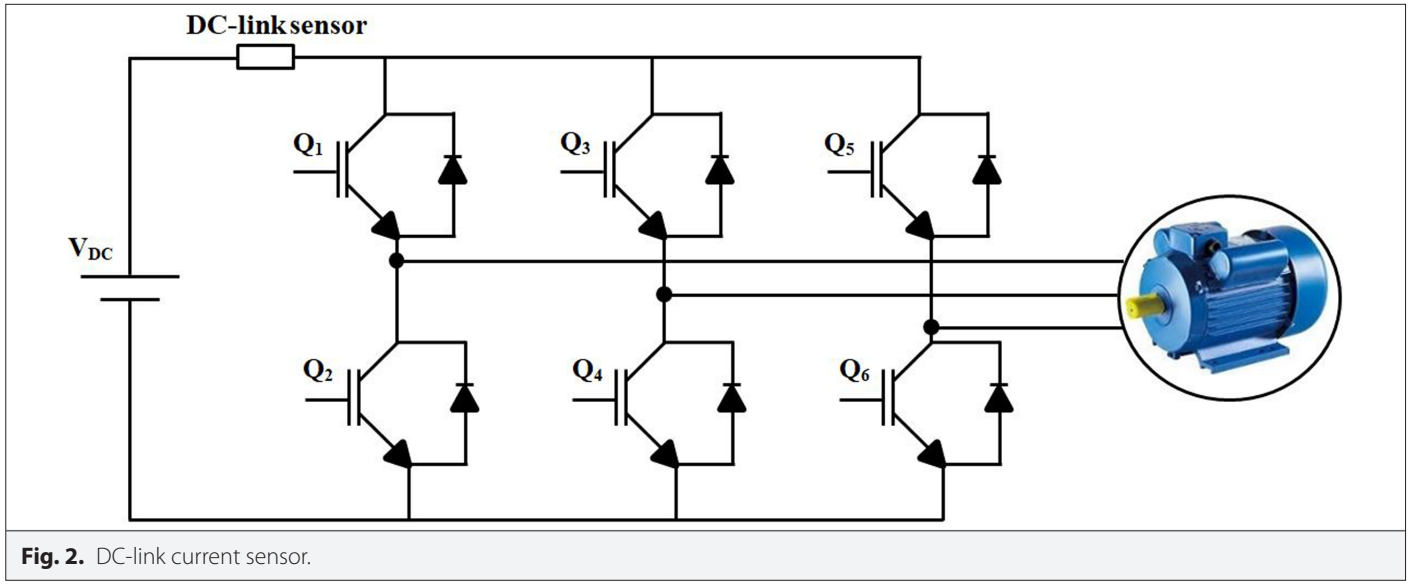

Fig. 2. DC-link current sensor.

III. DC-LINK MEASUREMENT METHOD

In order to carry out vector control of PMSM, the currents flowing from the stator windings must be determined. In this study, these currents were determined with DC-link current sensor and two different curve-fitting algorithms. Inverter circuit and DC-link current sensor connection are given in Fig. 2. Only one current value is measured with the DC-link current sensor. According to the voltage vectors applied to the inverter, the phase to which this DC-link current belongs to can be determined. Table II shows which phase current is measured in each voltage vector.

As it can be seen in Table II, only the current of a single phase can be specified with the DC-link current sensor, and the phase of this current changes according to the applied voltage vector. Curve-fitting methods can be used to determine the current values of other phases. In this study, the mean value method and the least squares method were used to fit the curve for determining other phase currents.

In Fig. 3, voltage vector plane is divided into three areas, which are low modulation area, sector boundary area, and measurable area. In order to reconstruct the phases current, DC-link current must be measured at least two times in a cycle. In sector modulation area, just an active voltage vector is active. Additionally, in low modulation region, DC-link current cannot be measured because of zero voltage vectors.

TABLE II. DC-LINK CURRENTS AND VOLTAGE VECTORS

Voltage Vector	S_a	S_b	S_c	I_{dc}
V_0	0	0	0	0
V_1	0	0	1	i_a
V_2	0	1	0	$-i_c$
V_3	0	1	1	i_b
V_4	1	0	0	$-i_a$
V_5	1	0	1	i_c
V_6	1	1	0	$-i_b$
V_7	1	1	1	0

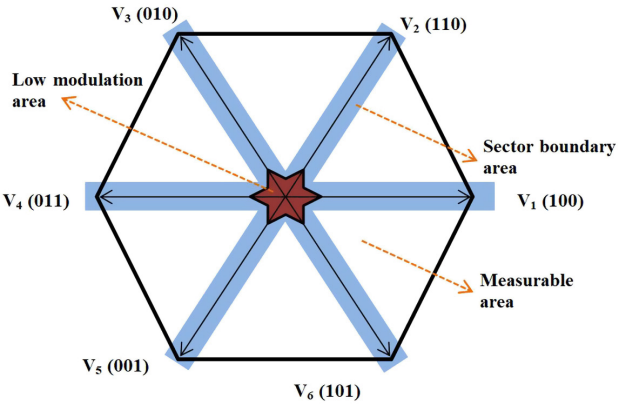

Fig. 3. Voltage vectors and immeasurable areas.

A. Mean Value Method

In this method, the current value of one of the phases is determined according to Table II. The current value of the other two phases is calculated using the average of the last five values of that phase. For example, if the V_2 voltage vector is applied, the i_c current is measured by the DC-link sensor. In this case, i_b current can be determined as follows with mean value method:

$$i_b^{k+1} = \frac{\left(i_b^k + i_b^{k-1} + i_b^{k-2} + i_b^{k-3} + i_b^{k-4}\right)}{5} \tag{8}$$

The following equation is used for the current value of the other phase (i_a). In this way, three phase currents are calculated:

$$i_a + i_b + i_c = 0 \tag{9}$$

Similarly, phase currents can be found if other voltage vectors are applied. For example, if V_3 voltage vector is applied, i_b current is measured by the DC-link sensor, and i_a and i_c can be calculated analytically using (8) and (9).

B. Least Squares Method

This method, developed by mathematician C. F. Gauss (1795), was used for the first time in determining the trajectory of Ceres asteroid in 1801 and was published for the first time in 1809 in the second volume of Gauss's collections. French mathematician A. Legendre in 1805 and American mathematician R. Adrain discovered the same method independently and unaware of Gauss in 1808. The least squares method is used for curve fitting in many areas.

In this method, the current value of one of the phases is determined according to Table II. The current value of the other two phases is calculated using the least squares method. For example, if the V_2 voltage vector is applied, the i_c current is measured by the DC-link sensor. In this case, i_b current can be determined as follows with the curve equation to be obtained as a result of curve fitting [27]:

$$i_b(t_k) = a_0 + a_1 t_k \tag{10}$$

By the definition of the least squares method:

$$E = \sum_{k=1}^{n} \varepsilon_k^2 \tag{11}$$

$$E = \sum_{k=1}^{n} \left[i_b(t_k) - f_k \right]^2 \tag{12}$$

$$E = \sum_{k=1}^{n} \left[a_0 + a_1 t_k - i_b(t_k) \right]^2 \tag{13}$$

In these equations, ε is the current error value, and E is the sum of the squares of these errors. If value of E is minimized according to a_0 and a_1, the following expressions are obtained:

$$\sum_{k=1}^{n} i_b(t_k) = a_0 n + a_1 \sum_{k=1}^{n} t_k \tag{14}$$

$$\sum_{k=1}^{n} i_b(t_k) t_k = a_0 \sum_{k=1}^{n} t_k + a_1 \sum_{k=1}^{n} t_k^2 \tag{15}$$

Using (14) and (15), a_0 and a_1 values are calculated, and the curve fitting is made up. Consequently, value of $i_b(t_{k+1})$ can be determined using (10). In addition, i_c can be determined using (9).

C. Performance Evaluation of Current Reconstruction Using Total Harmonic Distortion and Integral Squared Error

After applying FOC to PMSM with the DC-link current sensor and to test the success of the curve-fitting methods used, total harmonic distortion (THD) value of PMSM's phase currents can be used. The THD value of a signal can be calculated as follows:

$$\mathrm{THD} = \sqrt{\frac{\sum_{2}^{n} i_h^2}{i_1^2}} \times 100\% \,. \tag{16}$$

In addition to the THD, the ISE value can be calculated by taking the difference between reconstructed currents and the real phase currents flowing through the windings. Using an error signal, the ISE value can be calculated as follows:

$$\mathrm{ISE} = \int_0^{\infty} \left(i_{act}(t) - i_{rec}(t) \right)^2 dt \,. \tag{17}$$

IV. SIMULATION RESULTS

In this study, the simulation of the circuit given in Fig. 1 was performed. In this simulation, the values of the phase currents required for FOC were determined by DC-link current sensor shown in Fig. 2 and curve-fitting methods. Average value and least squares method were applied as curve-fitting methods. PMSM was operated with nominal speed and torque values, and phase current graphs were obtained. Fig. 4 shows the DC-link reconstructed currents, and Fig. 5

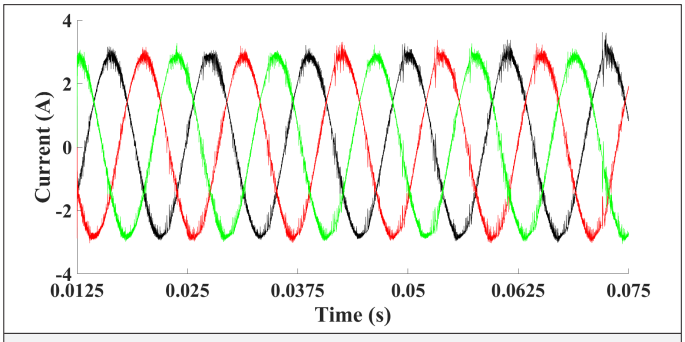

Fig. 4. Reconstructed phase currents using mean value method.

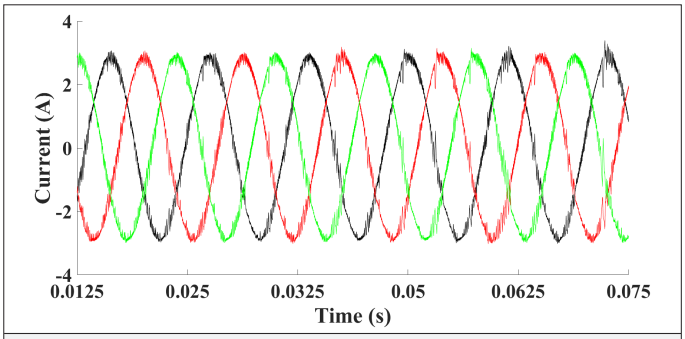

Fig. 5. Actual phase currents using mean value method.

shows the graphs of the real phase currents obtained by applying the mean value method.

Fig. 6 shows the DC-link reconstructed currents, and Fig. 7 shows the graphs of real phase currents obtained by applying the least squares method.

The graph of the current of phase aobtained as a result of both curve fitting methods is given in Fig. 8. As it can be seen in Fig. 8, it is clear that the ripple in some regions of the current graph obtained by the mean value method is higher than the least squares method. These ripples should be minimal, as they damage the battery.

In order to compare the two methods, harmonic analysis of the real phase currents obtained as a result of the application of both methods has been done. The THD values for both methods are given in Table III.

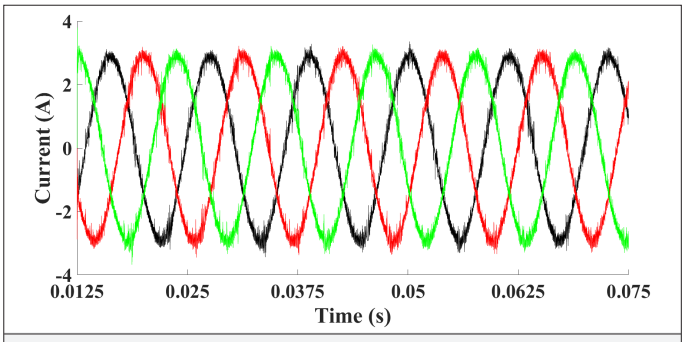

Fig. 6. Reconstructed phase currents using least squares method.

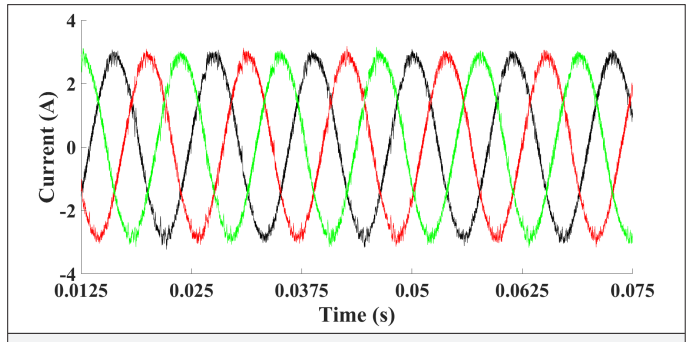

Fig. 7. Actual phase currents using least squares method.

As can be seen from Table III, the THD values of the currents of phases a and c and induced torque (T_e) are lower in the least squares method and close to sensored method (real current value). The THD value of phase b is approximately equal for two curve-fitting methods. Based on THD values, it can be said that the least squares method is more successful than mean value method.

In addition to the THD values, the current error was calculated using the difference between the reconstructed currents and actual values, and using these error values, ISE values for the two curve fitting methods are calculated and given in Table III. According to Table III, the values of the phase currents estimated by the least squares method are closer to the values of the actual phase currents. In addition, error between reference and induced torque is smaller for least squares method than mean value method. Considering both harmonic analysis and ISE values, both methods seem to be successful. In addition, when both THD and ISE values are taken into consideration, it can be said that the least squares method is more successful than the average value method.

In addition to current graphs, torque and speed graphs for both curve fitting methods are given in Fig. 9 and Fig. 10. When Fig. 9 is analyzed, it is seen that there are large ripples in the torque graph obtained as a result of applying the mean value method. When Fig. 10 is analyzed, the speed graph obtained by applying the least squares method is closer to the reference speed. The least squares method in both graphs gave better results than the mean value method.

V. CONCLUSION

In this study, FOC of PMSM was successfully realized using only DC-link current sensor. Only one phase current was measured instantly, and

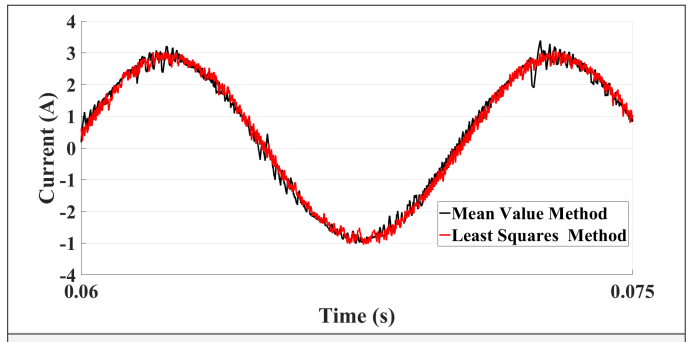

Fig. 8. Phase a current of PMSM.

TABLE III. TOTAL HARMONIC DISTORTION (THD) AND INTEGRAL SQUARED ERROR (ISE) VALUES

	THD			ISE	
Method/Phase	**Mean Value Method**	**Least Squares Method**	**Sensored Method**	**Mean Value Method**	**Least Squares Method**
i_a	7.8154	6.9331	6.126	84.485×10^3	84.429×10^3
i_b	8.1173	8.2087	7.935	85.689×10^3	85.62×10^3
i_c	7.2031	6.956	6.518	85.689×10^3	85.62×10^3
T_e	40.869	38.573	35.328	1.18×10^5	1.1795×10^5

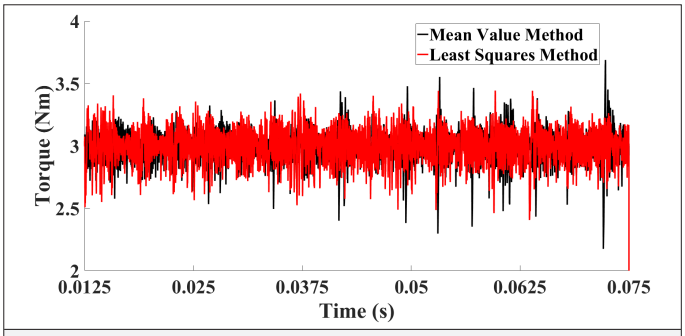

Fig. 9. Torque of PMSM.

the other two phase currents were predicted by using two methods. Using two different current reconstruction methods, the three phase currents required for the FOC were obtained with the DC-link current sensor. Thus, the number of current sensors to be used for vector control of PMSM and cost of sensors are reduced. When the phase currents obtained in the applied current reconstruction methods are compared with the real phase currents, it is observed that the performance of two methods is high. Thus, two different, simple, and highly applicable current reconstruction methods that can be used in DC-link applications with high performance have been proposed. Considering simulation results obtained from both methods and the THD and ISE values of these currents, the least squares method is seen to be more successful. Also, as it can be seen from the torque and speed graphs, the least squares method gives better results than the average value method. ISE and THD values of the induced torque also support this assessment. In obtained results, it is seen that only THD value of phase b current is insufficient. In future studies, methods with lower THD can be developed and applied. Also, by obtaining a lower ISE value, the difference between actual and estimated current can be reduced. In the motor speed graph, the results were very close to the performance of two current sensors.

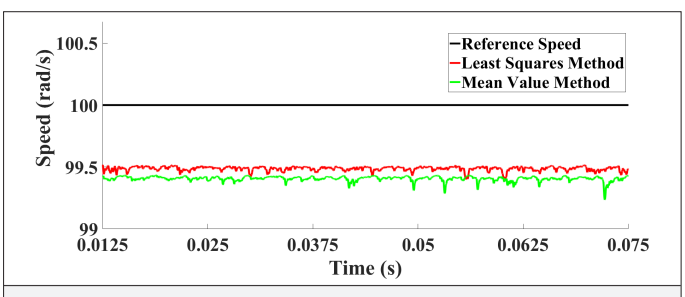

Fig. 10. Speed of PMSM.

Peer-review: Externally peer-reviewed.

Author Contributions: Concept – M.A., B.Ç.; Design – M.A., B.Ç.; Data Collection and/or Processing – M.A., B.Ç.; Analysis and/or Interpretation – M.A., B.Ç.; Literature Search – M.A., B.Ç.; Writing Manuscript – M.A., B.Ç.; Critical Review – M.A., B.Ç.

Conflict of Interest: The authors have no conflicts of interest to declare.

Financial Disclosure: The authors declared that this study has received no financial support.

REFERENCES

1. O. Saadaoui, A. Khlaief, A. Chaari and M. Boussak, "A new approach rotor speed estimation for PMSM on sliding mode observer," *J. Autom. Syst. Eng.*, vol. 9, pp. 66–78, 2015.
2. L. Harnefors, S. E. Saarakkala and M. Hinkkanen, "Speed control of electrical drives using classical control methods," *IEEE Trans. Ind. Appl.*, vol. 49, no. 2, pp. 889–898, 2013.
3. M. Abassi, A. Khlaief, O. Saadaoui, A. Chaari and M. Boussak, "Performance analysis of FOC and DTC for PMSM drives using SVPWM technique," in 2015 16th Int. Conf. Sci. Tech. Autom. Control Comput. Eng. (STA), Monastir, Tunisia, 2015, pp. 228–233.
4. V. M. Bida, D. V. Samokhvalov and F. S. Al-Mahturi, "PMSM vector control techniques: A survey." in 2018 IEEE Conference of Russian Young Researchers in Electrical and Electronic Engineering, Moscow, 2018, pp. 577–581.
5. A. Kronberg, "*Design and Simulation of Field Oriented Control and Irect Torque Control for a Permanent Magnet Synchronous Motor with Positive Saliency*," M.S. thesis, Maj., Uppsala University, Uppsala, Sweden, 2012.
6. M. Sebba, S. Hassaine, S. Moreau and A. Chaker, "Analyse et synthèse d'une structure de contrôle vectoriel simplifiée associée au couple de charge appliquée au moteur synchrone à aimant permanents," *Acta Electrotechn.*, vol. 50, no. 2, 2009.
7. G. Chandaka and G. Prasanth, "Direct torque control and field oriented control of PMSM using SVPWM Technique," *Int. J. Adv. Res. Sci. Eng.*, vol. 3, no. 11, pp. 274–283, 2014.
8. Z. Boulghasoul, A. Elbacha and E. Elwarraki, "*Performance of Fuzzy Anti Windup Compensator for PI Type Speed Controller in IM Drives*," in The 2nd International Conference on Industriel Systems and Logisitics, 2010.
9. Z. Boulghasoul, A. Elbacha, E. Elwarraki and D. Yousfi, "*Combined Vector Control and Direct Torque Control and Experimental Review and Evaluation*," in International Conference on Multimedia Computing and Systems, 2011, pp. 1–6.
10. F. Blashke, "A new method for the structural decoupling of a A.C. induction machines," in Conf. Rec. IFAC, 1971, pp. 1–15.
11. D. Casadei, F. Profurno, G. Serra and A. Tani, "FOC and DTC: Two viable schemes for induction motors torque control," *IEEE Trans. Power Electron.*, vol. 17, no. 5, pp. 779–787, 2002.
12. B. Wu, "*High-Power Converters and AC Drives*," IEEE Press, 2006.

13. Y. Xu, H. Yan, J. Zou, B. Wang and Y. Li, "Zero voltage vector sampling method for PMSM three-phase current reconstruction using single current sensor," *IEEE Trans. Power Electron.*, vol. 32, no. 5, p. 3797–3807, 2017.
14. Y. Cho, T. Labella and J. S. Lai, "A three-phase current reconstruction strategy with online current offset compensation using a single current sensor," *IEEE Trans. Ind. Electron.*, vol. 59, no. 7, p. 2924–2933, 2012.
15. M. Pacas, "Sensorless drives in industrial applications," *IEEE Ind. Electron. Mag.*, vol. 5, no. 2, pp. 16–23, 2011.
16. W. Jiang and B. Fahimi, "Current reconstruction techniques for survivable three-phase PWM converters," *IEEE Trans. Power Electron.*, vol. 25, no. 1, pp. 188–192, 2010.
17. U. Rieder, M. Schroedl and A. Ebner, "Sensorless control of an external rotor PMSM in the whole speed range including standstill using DC-link measurements only," in 2004 IEEE 35th Annual Power Electronics Specialists Conference, Aachen, Germany, vol. 2, 2004, pp. 1280–1285, IEEE Cat. No. 04CH37551. [CrossRef]
18. A. Piippo, K. Suomela, M. Hinkkanen and J. Luomi, "Sensorless PMSM drive with DC-link current measurement," in 2007 IEEE Industry Applications Annual Meeting, New Orleans, LA, 2007, pp. 2371–2377. [CrossRef]
19. H. Yeom, H. Ku and J. Kim, "Current reconstruction method for PMSM drive system with a DC link shunt resistor," in 2016 IEEE Energy Conversion Congress and Exposition (ECCE), Milwaukee, WI, 2016, pp. 1–6. [CrossRef]
20. A. Ahmed, Y. Sozer and M. Hamdan, "Maximum torque per ampere control for buried magnet PMSM based on DC-link power measurement," *IEEE Trans. Power Electron.*, vol. 32, no. 2, pp. 1299–1311, 2017. [CrossRef]
21. A. Kraemer, V. Heusinger, S. Schad and A. Ali, "Sensorless vector control of PMSM with observer-based phase current reconstruction using only a DC-link current sensor," in IEEE International Symposium on Sensorless Control for Electrical Drives (SLED), Catania, 2017, 2017, pp. 145–150. [CrossRef]
22. H. Li, Y. Qian, S. Asgarpoor and H. Sharif, "PMSM current sensor FDI based on DC link current estimation," in 2018 IEEE 88th Vehicular Technology Conference (VTC-Fall), Chicago, IL, USA, 2018, pp. 1–5. [CrossRef]
23. J. Lu, X. Zhang, Y. Hu, J. Liu, C. Gan and Z. Wang, "Independent phase current reconstruction strategy for IPMSM sensorless control without using null switching states," *IEEE Trans. Ind. Electron.*, vol. 65, no. 6, pp. 4492–4502, 2018.
24. W. Wang et al., "New three-phase current reconstruction for PMSM drive with hybrid space vector pulsewidth modulation technique," *IEEE Trans. Power Electron.*, vol. 36, no. 1, pp. 662–673, 2021.
25. Y. Yue, R. Zhang, B. Wu and W. Shao, "Direct torque control method of PMSM based on fractional order PID controller," in IEEE 6th Data Driven Control and Learning Systems Conference, 2017, pp. 411–415.
26. D. Y. Ohm, J. W. Brown and V. B. Chava, "Modeling and parameter characterization of permanent magnet synchronous motors," in Annual Symposium of Incremental Motion Control Systems and Devices, 1995, pp. 81–86.
27. T. P. Ryan, "*Modern Regression Methods*," New York: John Wiley Sons, 1997.

Mustafa Aktaş received the BSc, MSc, and PhD degrees in Electrical and Electronics Engineering from Karadeniz Technical University, Trabzon, Turkey, in 1992, 1998, and 2006, respectively. He studied a Postdoctoral researcher in Electrical and Computer Engineering, Texas A&M University, Texas, USA, between 2010 and 2011. He is currently an associate professor in the Department of Electrical and Electronics Engineering, Ondokuz Mayis University, Samsun, Turkey. His research interests include AC motor drives and control and electric and hybrid electric vehicles.

Barış Çavuş received the BSc degree in Electrical and Electronics Engineering from Karadeniz Technical University, Trabzon, Turkey, in 2015, MSc in Electrical and Electronics Engineering from Ondokuz Mayis University, Samsun, in 2019 Turkey, and currently continues his PhD education at Ondokuz Mayis University. His research interests include AC motor drives and control and electric vehicles and machines design.